



Local Multilevel Threshold filtering in the curvelet domain

A. P. de Franco* (LENEP/UENF) and F. S. de Moraes (LENEP/UENF)

Copyright 2015, SBGf - Sociedade Brasileira de Geofísica

This paper was prepared for presentation during the 14th International Congress of the Brazilian Geophysical Society held in Rio de Janeiro, Brazil, August 3-6, 2015.

Contents of this paper were reviewed by the Technical Committee of the 14th International Congress of the Brazilian Geophysical Society and do not necessarily represent any position of the SBGf, its officers or members. Electronic reproduction or storage of any part of this paper for commercial purposes without the written consent of the Brazilian Geophysical Society is prohibited.

Abstract

Seismic reflection images are usually corrupted by different kinds of undesirable noise, which may compromise the interpretation process. Noise can be classified as coherent or incoherent. The Curvelet Transform (CT) is a relatively recent tool that brings the image to a higher dimension sparse domain with multiscale and multidirectional expansions. This transform lends itself particularly well to represent features that are smooth along a curve and have an oscillatory behavior in the normal direction, just like the main features of a seismic data. The higher sparsity promoted by CT allows that a few large coefficients represents the signal components while incoherent energy, like random noise, is spread amongst a great number of small coefficients. Additionally multidirectional decomposition turns out as a powerful feature in the analysis of seismic events, which have preferred directions. In this work is presented the development of a threshold estimate based on a windowed neighborhood Root Mean Square (RMS) that works as a weight array for curvelets coefficients at each location, and consequently, at each scale and direction.

Introduction

The filtering of seismic images is an important step to prepare seismic data to be utilized efficiently in other stages like interpretation or inversion. The CT is presented as a time-frequency tool with directional characteristics that enhances the sparsity, providing an optimal domain for filtering, where a few large coefficients represents the signal components (Candés & Donoho, 2000; Candès et al., 2006).

The CT is a tool similar to Wavelet Transform (Mallat, 1989), but with an additional directional decomposition feature. Also the curvelet coefficients fit better to smooth curves with an oscillatory behavior on their normal direction. Hence we believe that the CT is a better choice to decompose seismic images for filtering.

Thanks to the promotion of sparsity diverse threshold estimates were developed over these transforms in the last decades. Two of them are the *VisuShrink* (Donoho & Johnstone, 1994) and the *Classical Shrinkage Threshold* (CST) developed by Starck et al. (2002) and named in this manner by Bao and Li (2011), defined as

$$\lambda = \sigma \sqrt{2 \ln(N)}, \quad (1)$$

and

$$\lambda_{j,l} = \alpha \sigma E_{j,l}, \quad (2)$$

respectively, where σ represents the standard deviation estimated for the incoherent noise, N is the number of pixels, j and l are the scale and angle index respectively, E is a constant normalization factor, $\alpha = 4$ to the finest scale coefficients and $\alpha = 3$ otherwise. These methods are universal, where only one λ is utilized for all coefficients (In equation 2 the j and l index are indicated because the normalization factor). Other estimates techniques are called adaptive, where the threshold varies according to the scales and/or angles. The *BayesShrink* (Chang et al., 2000) is written as

$$\lambda_j = \frac{\sigma^2}{\sigma_x(j)}, \quad (3)$$

where σ^2 is the noise variance and $\sigma_x(j)$ is the standard deviation of the noise-free curvelet coefficients at a scale panel j . The $\sigma_x(j)$ can be estimated as

$$\hat{\sigma}_x(j) = \sqrt{\max(\hat{\sigma}_y^2(j) - \hat{\sigma}^2, 0)}, \quad (4)$$

where $\sigma_y(j)$ represents the standard deviation of the curvelets coefficients at a scale j . Another adaptive threshold technique is known as *SureShrink* (Donoho & Johnstone, 1995) and can be represented as

$$\text{SURE}(\lambda_j, d_{jk}) = N - 2\# [k : |d_{jk}| \leq \lambda_j] + \sum_{k=1}^N \min(|d_{jk}|, \lambda_j)^2, \quad (5)$$

and

$$\lambda_{j,\text{SURE}} = \operatorname{argmin}_{0 \leq \lambda_j \leq \sqrt{2 \ln(N)}} \text{SURE}(\lambda_j, d_{jk}), \quad (6)$$

where N is the number of coefficients, d_{jk} represents the coefficient value at a scale j and position k and $\#$ is the cardinality operator (the number of elements which satisfy a given condition). The above formulation looks for a λ_j which minimizes equation 5.

Observations made by the authors of *SureShrink* have led to the conclusion that the use of

$$\lambda_u = \sqrt{2 \ln(N)}, \quad (7)$$

known as universal threshold, works better for sparse situations when compared with the *SureShrink*. Therefore it was proposed to use a hybrid scheme that evaluates the sparsity of the coefficients panel via

$$S_d^2 = \frac{\sum_{k=1}^N (d_k^2 - 1)}{N} \quad \text{and} \quad \gamma_d = \frac{\log_2^{(3/2)}(N)}{\sqrt{N}}. \quad (8)$$

Hence the *SureShrink* threshold is selected according to the condition:

$$\lambda_j = \begin{cases} \lambda_{j, \text{SURE}}, & \text{if } S_d^2 \leq \gamma_d \\ \lambda_u, & \text{otherwise.} \end{cases} \quad (9)$$

These two methods, *BayesShrink* and *SureShrink*, were developed over the Wavelet Transform, which has no angular decomposition. However the application was extended here to CT, using the additional angular decomposition. When necessary, the estimation of the noise standard deviation was taken by

$$\hat{\sigma} = \frac{\text{median}[\lvert d^{(\text{finest})} \rvert]}{0.6745}, \quad (10)$$

where $d^{(\text{finest})}$ is a vector of the curvelet coefficients at the finest scale and 0.6745 is the median of the absolute values of a normal distribution.

In this work we developed a threshold estimate for the CT that is locally adaptive to the curvelet coefficients, and hence to the scales and directions, using a neighborhood RMS window. Our method was compared with *VisuShrink*, *CST*, *SureShrink* and *BayesShrink* when applied to a synthetic 2D data and finally we demonstrate the application of LMT on a real 2D seismic section.

Method

The development of a threshold technique that varies according to the location arrives on the characteristic of seismic images where the signal-to-noise ratio tends to decrease with time/depth due to attenuation of seismic waves. Thus in every coefficients panel of the curvelet domain a mobile window with the inverse RMS (since greater values of RMS tends to represent higher coefficients values that represents signals) is utilized as a weight array for the threshold estimate of each curvelet coefficient. The equation that represents the technique can be represented as

$$\lambda_{j,l}(k_1, k_2) = R \frac{A}{V_{j,l}(k_1, k_2)}, \quad (11)$$

and

$$V_{j,l}(k_1, k_2) = \sqrt{\frac{1}{N} \sum_{i=k_1-a}^{k_1+a} \sum_{j=k_2-b}^{k_2+b} C_{j,l}(i, j)^2}. \quad (12)$$

Here N represents the number of elements inside the window, a and b are half of the length and width of the window (rounded down) respectively, j and l are the scale and angle index of the curvelet coefficients C and k_1 and k_2 defines the location coordinates. The parameter R is a positive real value, empirically chosen, that regulates the intensity of the threshold. As the amplitudes of seismic data can vary depending on a scale factor and since the threshold is determined by a RMS value, we propose to rescale the seismic image, before application of CT, to a standard deviation of 180 and use a constant A equals to 10^3 . In this manner the sensitivity of the regulatory parameter R can result in a similar effect to different images. This threshold method was then named as *Local Multilevel Threshold* (LMT).

In order to make the LMT more flexible and adjustable to different types of seismic images, the parameter R can accept up to three different values. These values act in a complementary way, being applied under different conditions established by the user:

$$R = \begin{cases} R_f, & \text{if } j \geq E_{rf}, \\ R_a, & \text{if } j \geq E_{ra} \text{ and } \theta_1 \leq l \leq \theta_2, \\ R_g, & \text{otherwise,} \end{cases} \quad (13)$$

where E_{rf} and E_{ra} defines the scale panel from which will be applied the value R_f and R_a , respectively, and θ_1 and θ_2 defines the angular range in which the R_a value will be applied. These parameters are optional, and if not selected only the value R_g will be applied to all curvelet coefficients.

Once defined the threshold by the equation 11, the application is realized using the *Hard Threshold* operator:

$$D(Y, \lambda) = \begin{cases} Y, & \text{if } |Y| > \lambda, \\ 0, & \text{if } |Y| \leq \lambda. \end{cases} \quad (14)$$

Thus the application of LMT is given by:

$$C_{j,l}^{\text{Tr}}(k_1, k_2) = D(C_{j,l}(k_1, k_2), \lambda_{j,l}(k_1, k_2)), \quad (15)$$

where C represents the curvelet coefficients, C^{Tr} the curvelet coefficient after the application of the operator D and λ the threshold at a given scale j , angle l , and position k_1 and k_2 .

Results

The LMT method was compared with some of the classical methods cited previously. The efficacy of methods was evaluated through the PSNR (Peak Signal-to-Noise Ratio), where highest values means better quality, defined as

$$\text{PSNR}(x, y) = 20 \log \left(\frac{\text{MAX}}{\sqrt{\text{MSE}(x, y)}} \right), \quad (16)$$

and

$$\text{MSE} = \frac{1}{N} \sum_{i=1}^N (x_i - y_i)^2. \quad (17)$$

In the above equation N represents the number of pixels of image, x is the noise-free image, y is the result of filtering and MAX represents the maximum value that a pixel can receive, which can be calculated as $\text{MAX} = 2^B - 1$, where B is the number of bits per sample. The comparison between methods is presented on Figure 1. As can be seen the application of LMT resulted in the highest PSNR value when applied to the seismic noisy synthetic data, showing the best visual quality.

As real seismic data is frequently corrupted with a great variety of noise, the use of different values for the R parameter (using equation 13) can improve the results when properly chosen. These factors apply the LMT method with a different regulatory parameter for a determined scale and forward (R_f) and to a determined range of angle (R_a). Hence with a more complex

threshold, with three different values of R , the filtering of a real seismic section can be more flexible and better adjustable for an optimal result.

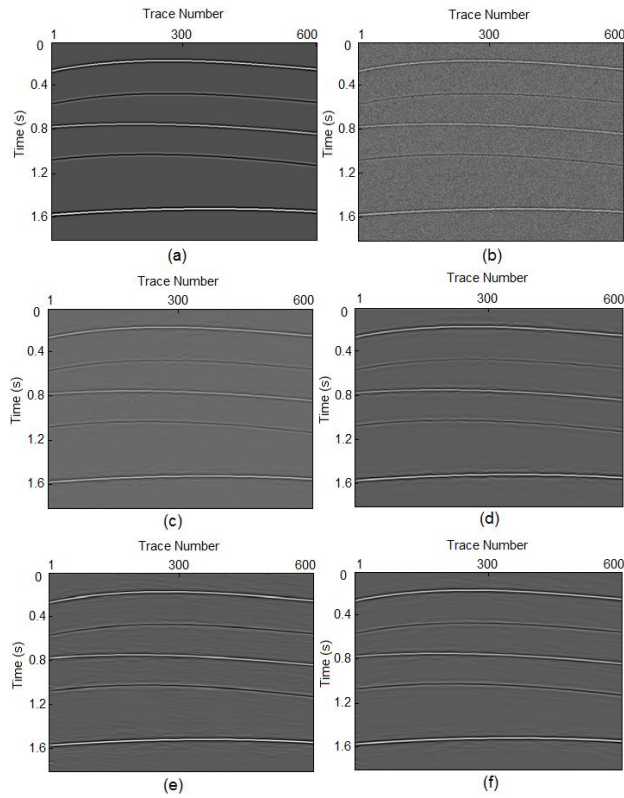


Figure 1: Results of a synthetic data filtering. a) Noise-free synthetic. b) Synthetic contaminated with a Gaussian noise with $\sigma = 30$ (PSNR of 27.04 db). c) CST denoise result (PSNR = 41.52). d) *SureShrink* denoise result (PSNR = 42.59). e) *BayesShrink* denoise result (PSNR = 43.89 db). f) LMT denoise result using $R = 1$ (PSNR = 44.19 db).

The application of LMT, utilizing three different values of R , was then tested in a real seismic section (Figure 2).

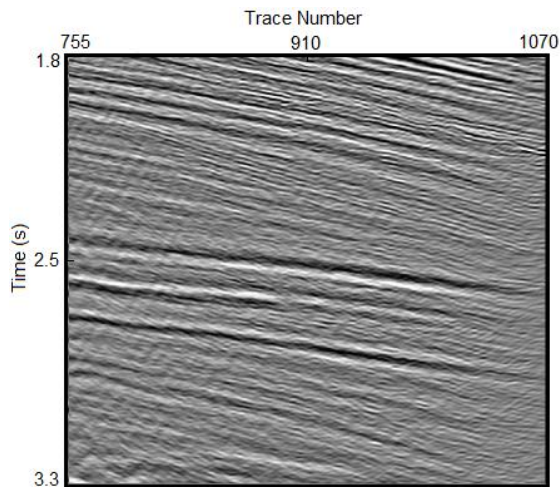


Figure 2: Real seismic section.

To better demonstrate the improvements of using three values for the parameter R , the filtering of Figure 2 was divided into three steps. In the first step the LMT was applied using $R = 3$. This value was taken as the highest before any signal loss after a few observations of different values. The result is shown on Figure 3.

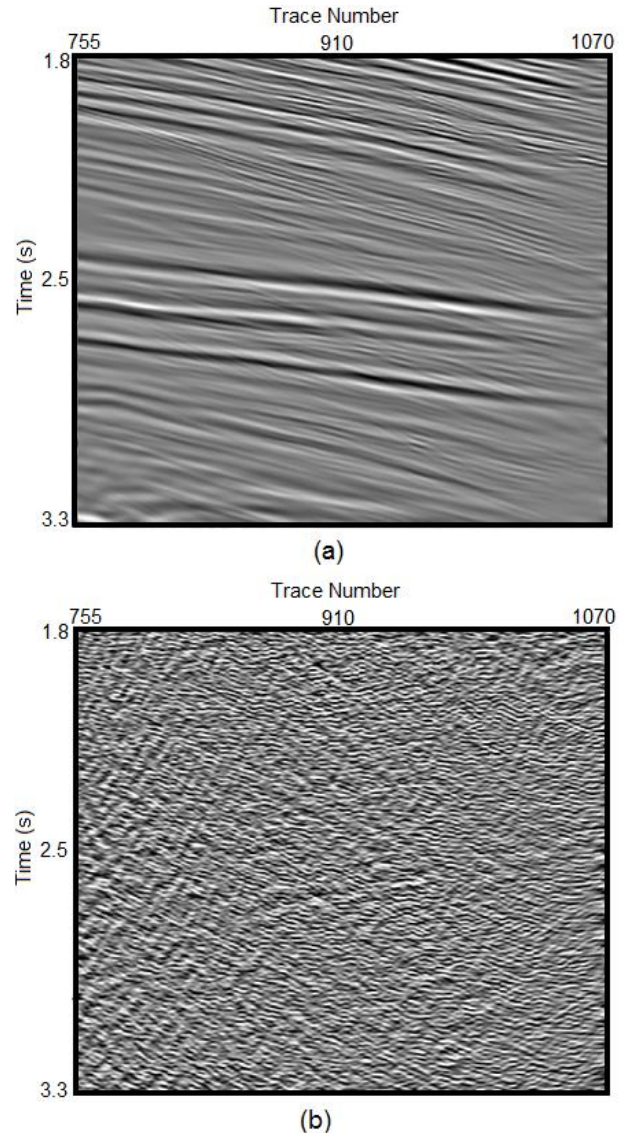


Figure 3: (a) Filtering result of Figure 2 utilizing $R = 3$. (b) Residue of the filtering.

When tested values of R higher than 3 the residue began to show signal components, which indicates a bad result. As can be observed Figure 3(a) still presents some noise that couldn't be removed utilizing only $R = 3$. This remaining noise features high frequency characteristics. Thus equation 13 was utilized with $R_g = 3$, $R_f = 10$ and $E_{ff} = 6$. In this case R_a was not used. With this configuration the threshold could be applied to the highest scales (up to six) with stronger value without compromise the lowest scales. The result utilizing these parameters is presented on Figure 4. As can be seen the high frequency noise was almost completely removed without compromising the signal components.

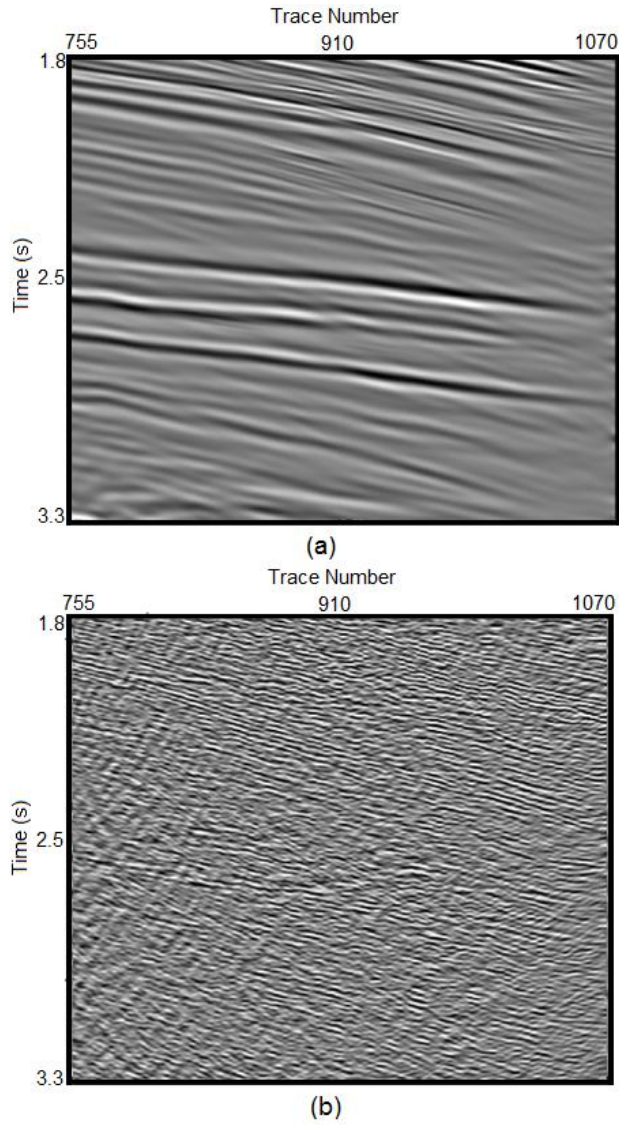


Figure 4: (a) Filtering result of Figure 2 utilizing $R_g = 3$, $R_f = 10$ and $E_{rf} = 6$. (b) Residue of the filtering.

In the third step of the process were utilized three different values for R :

$$R = \begin{cases} 10, & \text{if } j \geq 6, \\ 30, & \text{if } j \geq 6 \text{ and } 110^\circ \leq l \leq 160^\circ, \\ 3, & \text{otherwise.} \end{cases} \quad (18)$$

The above configuration adds the parameter $R_a = 30$, which is applied only up to the sixth scale and for the angular range 110° - 160° . This is a useful way to remove noise that contaminated the section only in some specific directions, taking advantage of the orientation decomposition of CT.

When equation 18 is utilized the LMT results in a visually better image than the original, with no signal loss compromising the data (Figure 5).

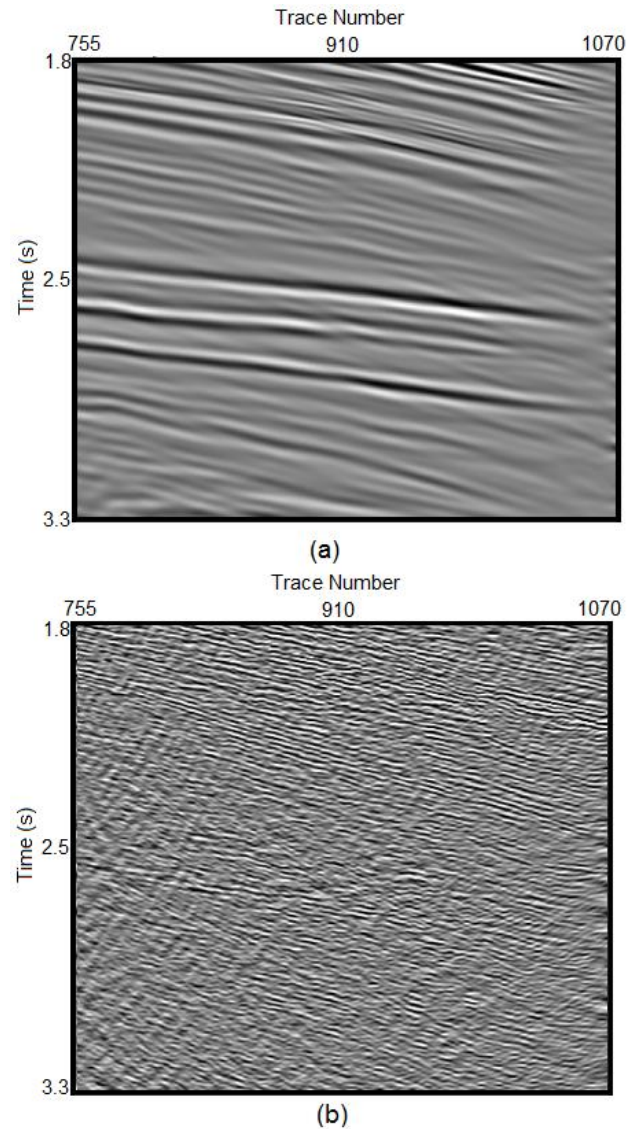


Figure 5: (a) Filtering result of Figure 2 utilizing $R_g = 3$, $R_f = 10$, $R_a = 30$, E_{rf} and $E_{ra} = 6$, $\theta_1 = 110^\circ$ and $\theta_2 = 160^\circ$. (b) Residue of the filtering.

Thus the application of LMT with three different values for the regulatory parameter is a better way to adjust the filtering for a real seismic data. A better way to adjust the parameters of LMT is start with only one parameter, $R_g = 1$ and then evaluate the filtering output and his residue. If the filtered result still noisy the R_g parameter must increase while no seismic signals can be observed in residue. If the result still noisy, and any increase in the parameter R_g leads to a signal loss, the optional parameters must be used to complement the filtering and improve results.

Conclusions

An optimal filtering of seismic data is an important step to be taken before an interpretation or a process that requires a clean image. The CT provides a high sparse domain with a scale and orientation decomposition, with atoms (curvelets) that fits very well to seismic waves.

Based on that a complex threshold that explore the orientation decomposition and the characteristic of seismic images, where SNR vary with time (depth), was here developed and applied to synthetic and real data.

The *Local Multilevel Threshold* method showed better results when compared with classical thresholds found on literature, like *VisuShrink*, *SureShrink*, CST and the *BayesShrink*. In addition to the highest PSNR, a better visual quality of LMT can be observed in the synthetic results.

To improve the flexibility of LMT, the regulatory parameter R may receive up to three different values that explore the scale and angular decomposition of CT. The variety of combinations is extensive, allowing to be adjusted to different types of seismic data.

The presentation of this threshold technique it's not a final stage of development. The concepts and results presented here show that a more complex threshold estimation, that explores all the characteristics of CT, must be the better way to filter seismic images.

Acknowledgments

We thank the members of Reservoir Inference Group (from portuguese GIR) of LENEPU/UENF-Brazil. We also thank PETROBRAS SA for the project funding to which this work is part.

References

- Bao, Q.; Li, Q., 2011 *Translation Invariant Denoising Using Neighbouring Curvelet Coefficients*. IEEE 978-1-4244-9857-4
- Candès, E. J.; Donoho, D. L., 2000 *Curvelets – A Surprisingly Effective Nonadaptive Representation For Objects with Edges*. Technical report, Stanford – CA, Department of Statistics, Stanford University
- Candès, E. J.; Demanet, L.; Donoho, D.; Ying, L., 2006 *Fast Discrete Curvelet Transform*. Applied and Computational Mathematics, Caltec, Pasadena. Department of Statistics, Stanford University
- Chang, M. V. S. G.; Yu, B., 2000 *Adaptative wavelet thresholding for image denoising and compression*. IEEE Transactions on Image Processing, 9(9), p. 1532 – 1546
- Donoho, D. L., 1995 *De-noising by soft thresholding*. IEEE Transactions on Information Theory, 41(3), p. 613 – 627
- Donoho, D. L.; Johnstone, I. M., 1994 *Ideal spatial adaptation via wavelet shrinkage*. Biometrika, 81, p. 425-455
- Mallat, S. G., 1989 *A theory for multiresolution signal decomposition: the wavelet representation*. IEEE Trans. Patt. Anal. Mach. Intell., 11, p. 674-693
- Starck, J. L.; Candès, E. J.; Donoho, D. L., 2002 *The curvelet transform for image denoising*. IEEE Trans. Image Process. Vol 11, 670-684